ACS OMEGA

Open Access

http://pubs.acs.org/journal/acsodf

Article

Metabolite Changes in Soybean (*Glycine max*) Leaves during the Entire Growth Period

Young Jin Park,[#] Jong Sung Lee,[#] Soyoung Park,[#] Ye Jin Kim, Vimalraj Mani, Kijong Lee, Soo Jin Kwon, Sang Un Park, and Jae Kwang Kim*

Cite This: *ACS Omega* 2023, 8, 41718−41727

Read Online

ACCESS | Metrics & More | Article Recommendations | Supporting Information

ABSTRACT: Although soybean (*Glycine max*) leaves generate building blocks to produce seeds, a comprehensive understanding of the metabolic changes in soybean leaves during the entire growth stages is limited. Here, we investigated the metabolite changes in soybean leaves from five cultivars among four vegetative (V) and eight reproductive (R) stages using metabolite profiling coupled with chemometrics. Principal component analysis (PCA) of all samples showed a clear separation by growth stage. The total amount of monosaccharides and organic acids for energy production were highly detected in the V stage samples, accumulating in concentrations 2.5 and 1.7 times higher than in the R stage samples, respectively. The results of partial least-squares-discriminant analysis (PLS-DA) revealed a clear separation from R1 to R5 by the first PLS, suggesting significant alterations in the metabolic networks up to R5. After flowering, the stage of seed formation, R5, was associated with lower levels of most amino acids and an accumulation of phytosterols. The negative correlation observed between amino acids and phytosterol levels suggests a sophisticated coordination between carbon and nitrogen metabolism in plant, ensuring and supporting optimal growth (r = −0.50085, P = 0.0001). In addition, R-stage samples had decreased monosaccharide levels, indicating redistribution to seeds and senescence-related metabolite changes. Thus, metabolite profiling coupled with chemometrics could be a useful tool for investigating alterations in metabolic networks during various plant growth and development stages. Furthermore, we observed variations in flavonoid contents among the different cultivars. The results could be a basis of further studies on the source−sink interactions in the plant system.

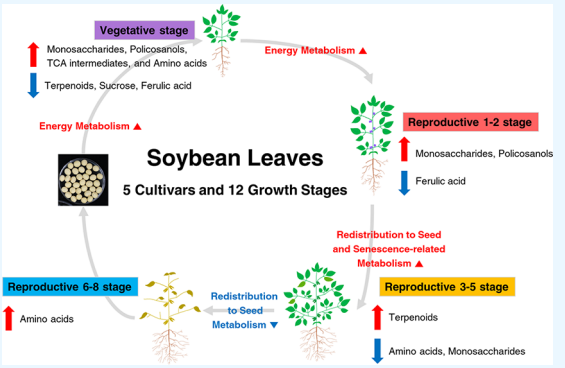

INTRODUCTION

Soybean (*Glycine max*) is an important food resource worldwide. Mature soybean seeds typically contain about 40% protein, 30% carbohydrates, 15% fat, 8% water, and other components.[1] Soybeans are a good source of protein for the human diet due to their high protein content.[2] In addition, soybean oil is highly praised for human consumption because it has a high content of unsaturated fatty acids.[2,3] Soybeans also contain high levels of flavonoids, particularly isoflavone.[4] Isoflavones have health benefits such as improving cardiovascular disease, relieving menopausal symptoms, and decreasing cancer incidence.[5] Soybean leaves are a rich source of flavonoid kaempferol and its derivatives. Kaempferol is effective against diabetes by regulating glucose homeostasis and lipid metabolism in mice (*Mus musculus*) and has shown anticancer and anti-inflammatory properties in humans due to its high antioxidant activities.[4,6−8] Although soybean leaves contain more flavonoids than seeds, soybean leaves are generally not harvested.[9,10]

Soybean growth is classified into the vegetative (V) and reproductive (R) stages.[11] The V stages are based on the number of trifoliate leaves. For example, V1 is the one-trifoliate-leaf stage while V2 is the two-trifoliate-leaf stage. The R stages reflect the periods of flowering, seed development, seed maturation, and senescence: R1 indicates the beginning of flowering, R2 represents full bloom, R3 represents the initial pod stage, R4 represents full pod, R5 represents the beginning of seed development, R6 represents full seeds, R7 indicates the beginning of seed maturity, and R8 represents full seed maturity.[11] Understanding the changes in the phytochemicals accumulating in soybean leaves over successive growth stages is important for determining their optimal harvest window. Several published studies have attempted to determine the optimal harvesting time of soybean leaves to harness the maximum health-promoting effects of their phytochemicals.[12−14] Most studies have focused on changes in flavonoid contents

Received: August 15, 2023
Revised: September 27, 2023
Accepted: October 10, 2023
Published: October 24, 2023

throughout the R stages. Recently, changes in compounds have been reported across multiple growth stages using nuclear magnetic resonance (NMR) imaging for a small number of growth stages and genotypes.[9,15]

Metabolomics is used to comprehensively describe complex metabolic changes by analyzing and identifying the metabolites in an organism at specific times or growth conditions.[16,17] Integrating analytical biochemistry and bioinformatics techniques is thus necessary for metabolite analysis.[18] Metabolomics has revealed metabolite changes over time in rice (*Oryza sativa*), barley (*Hordeum vulgare*), radish (*Raphanus sativus*), and soybean.[19−22] For example, Zhao et al. observed metabolic changes during seed germination in various barley varieties.[19] Similarly, Shu et al. characterized the metabolite profiles of germinating rice seeds in 24 h intervals.[21] Metabolome profiling of young radish sprouts was performed to observe metabolite changes in response to nitrogen deficiency.[22] Unlike previous short-term analyses, Jung et al. looked for the metabolic changes of soybean leaves collected from 8-, 12-, and 16-week-old plants of different genotypes.[20] These studies support the idea that metabolomics is an effective tool for observing metabolic changes in plants over time.

Extensive research has been conducted on soybean seeds due to their high value as food commodity. By contrast, soybean leaves have received less interest, although they are the primary sites of photosynthesis and experience changes in metabolite profiles that may help explain the differences between cultivars. To the best of our knowledge, few metabolomics-based approaches to soybean leaves have considered a comprehensive understanding of the entire growth stage.[9] The objective of this study was to analyze and compare the metabolites in the leaves of five different soybean cultivars across 12 growth stages using gas chromatography-time-of-flight-mass spectrometry (GC−TOF−MS), GC−quadrupole (q)MS, and ultraperformance liquid chromatography (UPLC)-MS/MS. Thus, we aimed to investigate alterations in metabolic networks associated with plant development throughout various growth stages of the soybean life cycle.

MATERIALS AND METHODS

Chemicals and Reagents. Daidzein, genistein, glycitein, squalene, ribitol, methoxyamine chloride, ascorbic acid, 6-methoxyflavone, pyridine, and *N*-methyl-*N*-trimethylsilyl trifluoroacetamide (MSTFA) were purchased from Sigma-Aldrich (St. Louis, Missouri, USA). Palmitic acid and stearic acid were purchased from Supelco (Bellefonte, Pennsylvania, USA). Methanol and ethanol were purchased from Daejung (Siheung, Republic of Korea). Chloroform was purchased from B&J (Burdick and Jackson, Muskegon, Michigan, USA). Hydrochloric acid and hexane were purchased from Fisher Scientific (Waltham, Massachusetts, USA). Potassium hydroxide was purchased from Wako (Wako Pure Chemical Corporation, Osaka, Japan). Dimethyl sulfoxide was purchased from Junsei (guaranteed reagent grade, Tokyo, Japan). All other chemicals used in this study were HPLC grade unless stated otherwise.

Soybean Sample Preparation. The five soybean (*G. max*) cultivars (DW, "Daewon"; IP, "Ilpum"; MS, "Miso"; KA, "Kwangan"; AR, "Aram") were cultivated at the National Institute of Crop Science in Jeonju, Korea (longitude: 127°02′ 27.2″ E; latitude: 35°49′ 45.6′′ N; altitude: 33.2 m) (Figure S1). These five cultivars belong to the soybean core collection group used for food in the Republic of Korea: MS for soy milk, DW for soybean paste and tofu, AR and KA for vegetables, and IP for black bean. DW and MS are yellow, large-sized seed soybeans that were registered in 2001 and 2020, respectively, with the National Agrobiodiversity Center (https://genebank.rda.go.kr (accessed on 20 September 2023)). KA and AR are yellow, small-size seed soybeans that were registered in 1995 and 2018, respectively, with the National Agrobiodiversity Center (https://genebank.rda.go.kr (accessed on 20 September 2023)). IP is black, large-size seed soybean that was registered in 1997 at the National Agrobiodiversity Center (https://genebank.rda.go.kr (accessed on 20 September 2023)). Each soybean cultivar was sown in an isolated greenhouse on May 27, 2022, and transferred to an isolated field on June 9, 2022. Planting was carried out in 50 cm intervals between seedlings on an 80 × 0.8 m row, with 20 seedlings planted for each soybean cultivar. Soybean plants were grown from June 9 to September 23, 2022, with the average temperature during the cultivation period being 25.6 °C and an average relative humidity of 70%. Samples were collected in three replicates at each growth stage following previously reported data on soybean growth stages.[11] Leaf samples were selected from undamaged leaves among the stems located at the second and third positions along the main stem during the V and R stages. Samples were immediately frozen and stored in liquid nitrogen; after freeze-drying, the samples were ground using a mortar and pestle and stored in a freezer (IBK-600F, Infobiotech Co., Ltd., Daejeon, Korea) at −20 °C.

Extraction and Determination of Hydrophilic Compounds by GC−TOF−MS. The extraction and determination of hydrophilic compounds were analyzed as previously described, with slight modifications.[23] An aliquot of 10 mg of ground leaf powder was placed in a 2 mL tube, to which 1 mL of methanol:water:chloroform (2.5:1:1, v/v/v) and 60 μL of ribitol (200 μg/mL in methanol) as an internal standard were added. After vortexing, the mixtures were shaken using a Thermomixer Comfort (model 5355, Eppendorf AG, Hamburg, Germany) at 1200 rpm for 30 min at 37 °C. The mixtures were centrifuged at 16,000 × *g* for 5 min at 4 °C. The supernatants (800 μL) were transferred to new 2 mL tubes and mixed with 400 μL of distilled water. The mixtures were centrifuged at 16,000 × *g* for 5 min at 4 °C. The resulting supernatants (900 μL) were then transferred to a new 2 mL tube. The solvent was evaporated for 4 h in a centrifugal concentrator (CVE-3110, EYELA, Tokyo, Japan) and then freeze-dried for over 16 h using a MCFD8512 freeze-dryer (IlShin Bio-Base Co., Ltd., Korea). For derivatization, the pellets were resuspended in 80 μL of 2% (w/v) methoxyamine hydrochloride in pyridine and shaken at 1200 rpm for 90 min at 30 °C on a Thermomixer Comfort. Thereafter, 80 μL of MSTFA was added to the mixtures and the mixtures were shaken at 1200 rpm for 30 min at 37 °C on a Thermomixer Comfort.

Hydrophilic compounds were analyzed using a Pegasus FLUX (LECO, St. Joseph, Michigan, USA) with an Rtx-5 ms column (30 m length, 0.25 mm diameter, and 0.25 μm thickness; Restek, Bellefonte, Pennsylvania, USA). The gas chromatography conditions were as follows. The temperatures of the inlet, transfer line, and ion source and the volume of injection were set to 230 °C, 280 °C, 250 °C, and 1 μL, respectively. Helium was used as the carrier gas with a column flow rate of 1.0 mL/min and an injection mode set to split mode with a 1:25 ratio. The GC oven program was held at 80 °C for 2 min, increased at a rate of 15 °C/min up to 320 °C, and held there for 10 min. Data were acquired over a *m*/*z* mass range of 85−600. For relative quantification, data were analyzed through Chroma TOF BT software (version 5.50.55, LECO, St. Joseph, Michigan, USA),

https://doi.org/10.1021/acsomega.3c06043
ACS Omega 2023, 8, 41718−41727

calculated as the peak area of each metabolite based on that of the internal standard. For annotation, the peaks were identified based on the mass spectral data by comparison to in-house libraries, NIST17, and Wiley9.

Extraction and Determination of Lipophilic Compounds by GC−qMS. The extraction and determination of lipophilic compounds were analyzed as previously described, with slight modifications.[24] Aliquots of 50 mg of soybean leaf powder were placed in a 15 mL conical tube, to which 3 mL of 0.1% (w/v) ascorbic acid in ethanol and 50 μL of 5α-cholestane in hexane (10 μg/mL) were added as an internal standard. After vortexing for 20 s, the mixtures were incubated in a water bath at 85 °C for 5 min. After 120 μL of potassium hydroxide (80%, w/v) was added for saponification, the samples were vortexed for 20 s and incubated in a water bath at 85 °C for 10 min. The mixtures were then immediately cooled on ice for 5 min, followed by adding 1.5 mL each of hexane and distilled water. After vortexing for 20 s, the mixtures were centrifuged at 1200 × *g* for 5 min at 4 °C. The resulting supernatants (1.5 mL) were transferred to a new 15 mL conical tube. To reextract any remaining compounds, 1.5 mL of hexane was added to the pellets from the first tube and the mixtures were then centrifuged at 1200 × *g* for 5 min at 4 °C. The supernatants (1.5 mL) were combined with the previous supernatants and evaporated in a centrifugal concentrator (CVE-3110, EYELA, Tokyo, Japan). For derivatization, the dried pellets were resuspended in 30 μL of MSTFA and 30 μL of pyridine and shaken at 1200 rpm for 30 min at 60 °C on a Thermomixer Comfort (model 5355, Eppendorf AG, Hamburg, Germany).

Lipophilic compounds were analyzed on a GCMS-QP2010 Ultra system (Shimadzu, Kyoto, Japan) attached to an AOC-20i autosampler (Shimadzu) with a Rtx-5 ms column (30 m length, 0.25 mm diameter, and 0.25 μm thickness; Restek, USA). The GC conditions were set as follows. The temperatures of the inlet, ion source, and interface and the volume of injection were set to 290 °C, 230 °C, 280 °C, and 1 μL, respectively. Helium was used as a carrier gas at a column flow of 1.0 mL/min and with an injection mode set to split mode with a 10:1 ratio. The GC oven program was held at 150 °C for 2 min, increased at a rate of 15 °C/min up to 320 °C, and held there for 10 min. The chromatograms and mass spectra were analyzed using Shimadzu LabSolutions GCMSsolution software version 4.20 (Kyoto, Japan). Qualitative and quantitative evaluations were conducted against the internal standards. The calibration curve range for each lipophilic compound was 0.025−5.00 μg, and a fixed concentration (0.50 μg each) of the internal standard was used.

Extraction and Determination of Flavonoid Compounds by UPLC−MS/MS. The extraction and determination of flavonoid compounds were analyzed as previously described, with slight modifications.[25] An aliquot of 25 mg of soybean leaf powder was placed in a 2 mL tube, to which 0.2 mL of 1.2 M hydrochloric acid in 80% (v/v) ethanol, 50 μL of 2.5 ppm galangin (flavonoid internal standard), and 0.5 ppm 6-methoxyflavone (isoflavone internal standard) were added. After vortexing, the mixtures were shaken at 1200 rpm for 120 min at 26 °C using a Thermomixer Comfort (model 5355, Eppendorf AG, Hamburg, Germany). The mixtures were centrifuged at 13,000 × *g* for 10 min at 25 °C using a centrifuge (MX-307, TOMY, Japan). The resulting supernatants were filtered through a 0.5 μm filter (13JP050AN, Advantec Toyo Roshi Kaisha Ltd., Tokyo, Japan). The filtered samples were then analyzed using an UPLC instrument (ACQUITY UPLC I-Class PLUS, Waters, Milford, Massachusetts, USA) coupled to a photodiode array detector and tandem mass spectrometer. An ACQUITY UPLC CSH C18 1.7 μm column (1.7 μm film thickness, 150 mm length, and 2.1 mm diameter, Waters, Milford, Massachusetts, USA) was equipped with the UPLC. The gradient eluents were carried out with 0.1% (v/v) formic acid in water (solvent A) and 0.1% (v/v) formic acid in acetonitrile (solvent B) at a constant flow rate of 0.3 mL/min. The linear gradient elution program was as follows: 0 min, 95% A; 0−20 min, 95−75% A; 20−28 min, 75−60% A; 28−30 min, 60−10% A; 30−32 min, 10−10% A; 32−35 min, 10−95% A; 35−40 min, 95−95% A (all percentages v/v). The injection volume was 1 μL. The column oven temperature was set to 30 °C. The UPLC system was connected to a Xevo micro Triple q MS (Xevo TQ-S micro, Waters, Milford, Massachusetts, USA) for analysis.

The mass spectrometer was operated in the positive ion mode. Nitrogen gas was used as the desolvation gas. The desolvation temperature was set to 500 °C at a rate of 1000 L/h with a source temperature of 120 °C. The capillary and cone voltages were set to 0.5 kV and 5 V, respectively. The collision gas energy for MS/MS was set to 15−30 V. The data were analyzed through the MRM mode. For the kaempferol group, quantification was carried out by proportional quantification through the ultraviolet−visible detection of kaempferol at 350 nm. For quantification estimation, the ratio of the relative peak area to that of the internal standard was determined based on the selected ions. The mass raw data were analyzed with the TargetLynx XS applications manager.

Statistical Analysis. All analyses were performed with biological replicates (at least three). Principal component analysis (PCA) and partial least-squares discriminant analysis (PLS-DA) (SIMCA-P version 13.0; Umetrics, Umeå, Sweden) were performed with data normalized with unit variance scaling to determine the relationships among the 72 detected compounds. Analysis of variance (ANOVA) and Pearson's correlation analysis were performed by using the SAS 9.4 software package (SAS Institute, Cary, North Carolina, USA). The bar graphs and heatmaps were generated using GraphPad Prism version 9.0.1 (GraphPad, Boston, Massachusetts, USA).

RESULTS AND DISCUSSION

Metabolite Profiling of Soybean Leaves during the Whole Growth Period. We analyzed soybean leaves collected at each of 12 growth stages from five cultivars (MS, DW, KA, IP, and AR) by GC−TOF−MS, GC−qMS, and UPLC−MS/MS. In total, we detected 43 hydrophilic compounds (Figure S2, Table S1), 15 lipophilic compounds (Figure S3, Table S2), and 14 flavonoid compounds (Figure S4, Table S3) in these samples.

We employed principal component analysis (PCA) to examine the metabolic changes that occurred during all stages of soybean leaf development. Accordingly, we performed a PCA using 72 metabolites detected above across the five soybean cultivars and 12 growth stages. The first two principal components (PC) of the PCA explained 39.9% of the total variance (PC1: 27.1%, PC2: 12.8%) (Figure 1A). V stages were located on the negative eigenvalue side of PC1. While we observed a clear separation between the V and R stages along PC1, a separation among the five cultivars was not apparent. As each point in the PCA plot represents one metabolite, we looked for metabolites that contribute to the separation of each sample by generating the corresponding loading plot (Figure 1B). The loading plot revealed higher levels of several metabolites in the V stages relative to the R stages: monosaccharides (xylose,

https://doi.org/10.1021/acsomega.3c06043
ACS Omega 2023, 8, 41718−41727

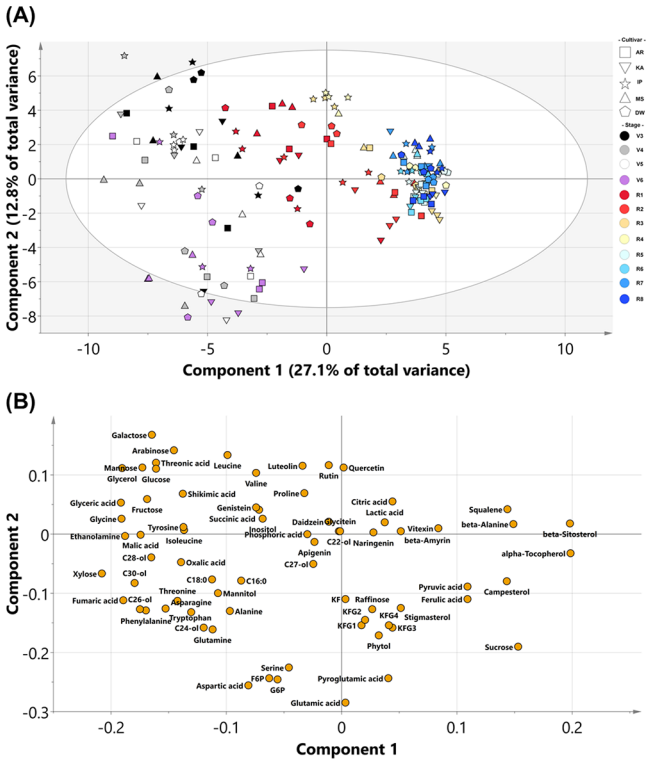

Figure 1. Data exploration of differentially abundant metabolites detected across 12 developmental stages and soybean cultivars. Principal component analysis (PCA) score plot (A) and loading plot (B) for all differentially abundant metabolites of soybean leaves over 12 growth stages. Abbreviations: F6P, fructose-6-phosphate; G6P, glucose-6-phosphate; C16:0, palmitic acid; C18:0, stearic acid; C22-ol, docosanol; C24-ol, tetracosanol; C26-ol, hexacosanol; C27-ol, heptacosanol; C28-ol, octacosanol; C30-ol, triacontanol; KF, kaempferol; KFG1, kaempferol 3-O-(2″-O-glucosyl-6″-O-rhamnosyl)-galactoside; KFG2, kaempferol 3-O-(2″-O-glucosyl-6″-O-rhamnosyl)-glucoside; KFG3, kaempferol 3-O-(2″-O-glucosyl)galactoside; KFG4, kaempferol 3-O-(2″-O-glucosyl)glucoside; DW, "Daewon"; IP, "Ilpum"; MS, "Miso"; KA, "Kwangan"; AR, "Aram".

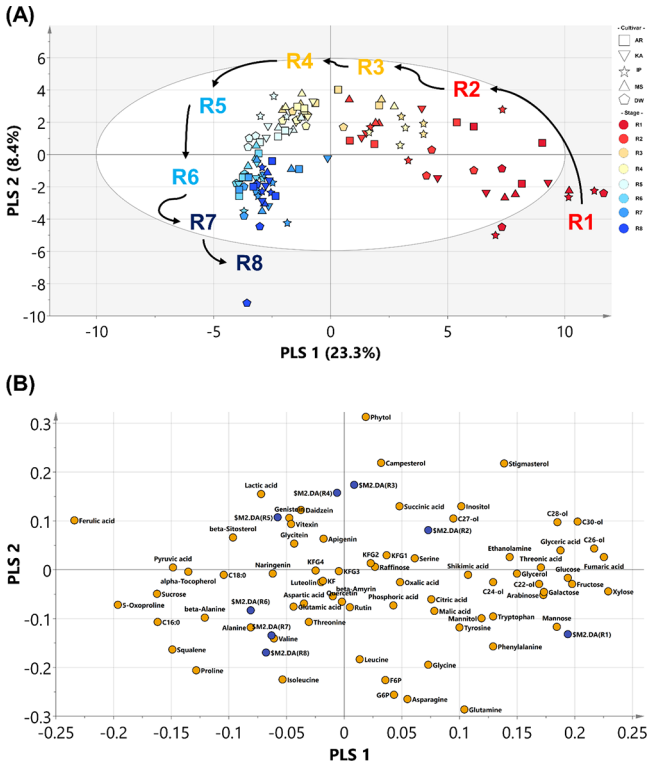

Figure 2. Data exploration of differentially abundant metabolites detected across the reproductive stages of soybean cultivars. Partial least-squares-discriminant analysis (PLS-DA) score (A) and loading plot (B) from differentially abundant metabolites from soybean leaves at the reproductive stage. Abbreviations: F6P, fructose-6-phosphate; G6P, glucose-6-phosphate; C16:0, palmitic acid; C18:0, stearic acid; C22-ol, docosanol; C24-ol, tetracosanol; C26-ol, hexacosanol; C27-ol, heptacosanol; C28-ol, octacosanol; C30-ol, triacontanol; KF, kaempferol; KFG1, kaempferol 3-O-(2″-O-glucosyl-6″-O-rhamnosyl)-galactoside; KFG2, kaempferol 3-O-(2″-O-glucosyl-6″-O-rhamnosyl)-glucoside; KFG3, kaempferol 3-O-(2″-O-glucosyl)galactoside; KFG4, kaempferol 3-O-(2″-O-glucosyl)glucoside; DW, "Daewon"; IP, "Ilpum"; MS, "Miso"; KA, "Kwangan"; AR, "Aram".

galactose, mannose, glucose, and fructose), policosanols (hexacosanol [C26-ol], octacosanol [C28-ol], and triacontanol [C30-ol]), organic acids (fumaric, glyceric, and malic acids), amino acids (phenylalanine, tryptophan, glycine, and threonic acids), and other components (glycerol and ethanolamine). Conversely, we noticed higher levels of terpenoids (beta-sitosterol, alpha-tocopherol, campesterol, and squalene), disaccharides (sucrose), organic acids (pyruvic acid and ferulic acid), and amino acids (bis(alanine)) in the R stages relative to V stages.

Energy metabolism is substantially higher in young leaves than that in mature leaves. Indeed, young leaves are actively growing and require a substantial and sustained amount of energy to support their metabolism. As a result, they tend to have higher rates of photosynthesis and respiration than mature leaves.[26,27] A previous study showed that monosaccharides are biosynthesized through photosynthesis in bean (*Phaseolus vulgaris*) leaves at an early stage while sucrose biosynthesis takes place in mature leaves.[20] In agreement, we detected many monosaccharides (xylose, galactose, mannose, glucose, and fructose) that are biosynthesized through photosynthesis and respiration during the V stages of soybean leaf development. Also during the V stages, energy metabolism was active, leading to an accumulation of tricarboxylic acid (TCA) cycle intermediates (fumaric and malic acid). Fatty acids, another metabolite with a high energy potential, are stored as triglycerides in plants. Indeed, we detected high levels of saturated fatty acids (palmitic acid [C16:0] and stearic acid [C18:0]) and glycerol in the V stages, indicating an active carbon-related energy metabolism. By contrast, the sucrose concentration was high during the R stages. This stage is characterized by the redistribution of carbohydrates from leaves to sink tissues, such as seeds, to support their maturation. Thus, the monosaccharides produced through photosynthesis are converted to sucrose by sucrose synthase and transported through the phloem.[28]

We also detected high contents of the wax component policosanol but low levels of ferulic acid in the V stages. Plants harness sunlight to power photosynthesis and fix carbon dioxide to produce glucose and release oxygen. For photosynthesis to occur, as with any biochemical reaction, plants require water. Wax is a lipid-based layer on the surface of leaves that helps to prevent excessive water loss through transpiration via the leaf epidermis. This waxy layer also decreases the amount of water lost, thereby increasing the water-use efficiency in plants. Thus, plants increase the biosynthesis of cuticular wax components

https://doi.org/10.1021/acsomega.3c06043
ACS Omega 2023, 8, 41718−41727

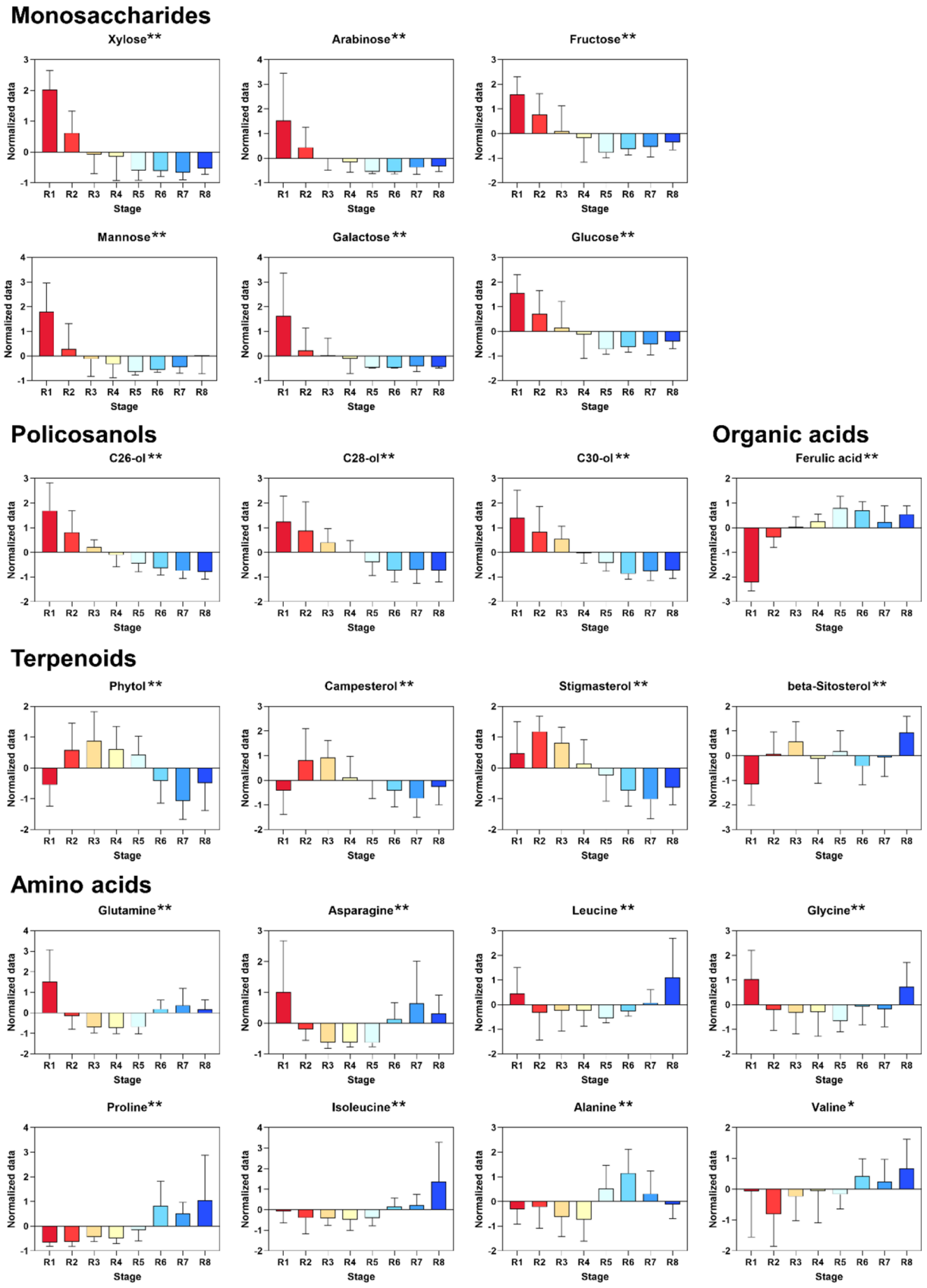

Figure 3. Relative quantification of representative differentially abundant metabolites across the reproductive stages. The relative concentration of each metabolite was normalized with unit variance scaling and was significantly different from stage to stage by analysis of variance (ANOVA) (* $p < 0.01$, ** $p < 0.001$). Abbreviations: C26-ol, hexacosanol; C28-ol, octacosanol; C30-ol, triacontanol.

https://doi.org/10.1021/acsomega.3c06043
ACS Omega 2023, 8, 41718−41727

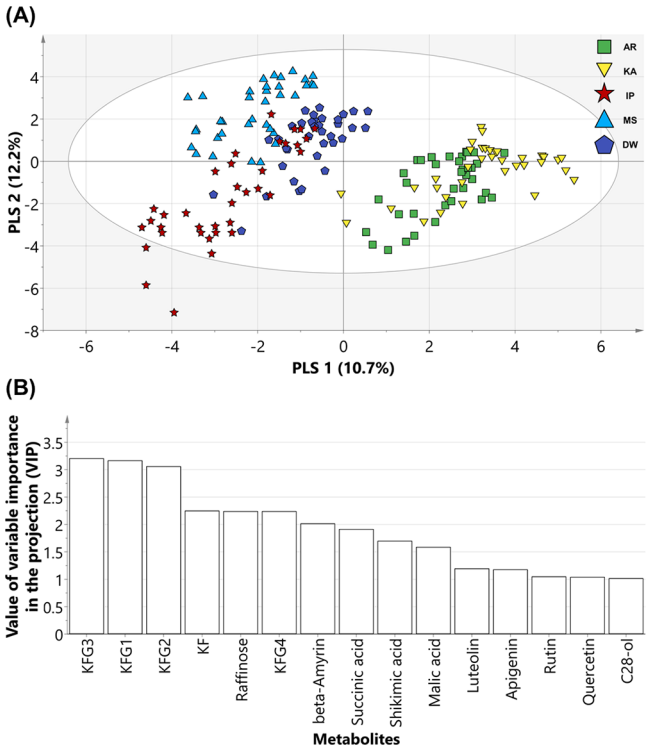

Figure 4. Data exploration of differentially abundant metabolites detected across soybean cultivars at all stages.

(such as policosanols) when faced with water stress to use water more efficiently.[29,30] Ferulic acid is a precursor of the secondary cell wall. The flowering hormone florigen increases the biosynthesis of secondary cell wall components, explaining the relatively high levels of ferulic acid observed in the R stages.[31] The levels of terpenoids (beta-sitosterol, alpha-tocopherol, campesterol, and squalene) increase in the R stages. Plants activate their secondary metabolism as they approach maturity, leading to an increase in terpenoid compounds.[20]

Soybean Leaves at the Reproductive Stages. During the V stages, the focus is primarily on the growth and production of new leaves. Notably, we detected no significant changes in metabolite contents among the V stages (Figure S5). The R stages comprise complex developmental transitions. During R1 and R2 the plant blooms, followed by pod formation in R3 and R4; finally, seeds fill during R5 and R6, culminating with plant and seed maturity at R7 and R8, and initiation of senescence. Unlike the V stages, the individual R stages lacked a clear separation in our PCA. We therefore turned to a PLS-DA, a supervised statistical analysis method that includes various group variables, to identify changes in metabolites according to each R(n) growth stage (Figure 2A). The first two components of PLS-DA explained 31.7% of the total variance (PLS1:23.3% and PLS2:8.4%). PLS1 was separated from the R1 to R5 stages, indicating significant metabolic network changes up to the R5 stage. The R1 and R2 stages had positive eigenvalues for PLS1, the R3 and R5 stages had a positive eigenvalue for PLS2, and the R6 and R8 stages had a negative eigenvalue for PLS2. These results indicate that PLS-DA successfully separated the R1 and R8 stages into three main groups.

The R1 and R2 stages showed an accumulation of monosaccharides (arabinose, fructose, galactose, glucose, mannose, and xylose) and policosanols (C26-ol, C28-ol, and C30-ol) and a decrease in ferulic acid (Figures 2B and 3). The R1−2 stages are temporally the closest to the V stages, marking the beginning of the reproductive phase when flowers bloom and thus before sugars are redistributed to seeds. As during the V stages, we detected high levels of metabolites related to energy metabolism (monosaccharides) and metabolites that contribute to the physical protection (policosanols) of plant tissues during the R1−2 stages.

The R3−5 stages were characterized by an accumulation of terpenoids (phytol, campesterol, stigmasterol, and beta-sitosterol) and a decrease in the levels of amino acids (glutamine, asparagine, isoleucine, proline, glycine, and leucine) and monosaccharides (xylose, fructose, mannose, galactose, arabinose, and glucose) (Figures 2B and 3). Especially, most of the terpenoids and amino acids were negatively correlated with each other, indicating that the carbon and nitrogen metabolism in plants is intricately coordinated to ensure and support optimal growth ($r = -0.50085$, $P = 0.0001$). R3−5 are the stages when the seedpod forms, and seed filling begins. Soybean seeds contain 40% protein, 30% carbohydrates, and 15% fat. During seed filling, sugars and amino acids biosynthesized in the leaves are transported to the seeds, redistributing the plant's nutrients. Consequently, the contents of sugars and amino acids decrease in the leaves during this period. Nitrogen transport in soybean starts with the assimilation of ammonium ions and their conversion to glutamine in roots, before organic nitrogen migrates through the phloem in the form of glutamine and asparagine.[32,33] Therefore, glutamine and asparagine are intricately involved in nitrogen redistribution to seeds; indeed, the contents of these two amino acids were much lower in leaves at the R3−5 stages. Additionally, secondary metabolism related to terpenoids increased in these stages. Phytosterol is also related to plant adaptation to temperature and response to pathogens.[34,35] Furthermore, as plants mature, they activate their secondary metabolism, which results in an increase in phytosterols.[20] Therefore, phytosterol, a senescence-related metabolite, was increased in R3−5 stages.

During the R6−8 stages, we observed the accumulation of amino acids (proline, isoleucine, valine, alanine, threonine, glutamic acid, aspartic acid, leucine, asparagine, and glutamine) (Figures 2B and 3). During stages R6 and R8, seed filling is completed and senescence is initiated. At these stages, several amino acids accumulate in seeds, among which the major ones are glutamic acid, aspartic acid, arginine, leucine, and lysine.[1,36] With the exception of lysine, the levels of these amino acids increased in the leaves at the R6 and R8 stages, indicating a trend of amino acid accumulation through their biosynthesis after the redistribution of nutrients from leaves to seeds is completed. Leucine, isoleucine, valine, and threonine are essential amino acids for humans. Isoleucine, valine, and leucine are branched-chain amino acids that support muscle movement in humans. Proline is not an essential amino acid but has health-promoting effects such as strengthening immunity, improving antioxidant status, and promoting intestinal health and nutrient uptake. Even though soybean leaves are discarded after seed harvest, soybean leaves in the R6−8 stages have the greatest potential for nutrition compared to other stages as they have higher contents of essential amino acids. Overall, we observed redistribution to seeds and senescence-related metabolite changes in the R stages: as the R stages progressed, amino acids and monosaccharides were redistributed to seeds, while terpenoid contents increased in leaves.

Partial least-squares-discriminant analysis (PLS-DA) score (A) and variable importance in projection (VIP) plot (B) from

https://doi.org/10.1021/acsomega.3c06043
ACS Omega 2023, 8, 41718−41727

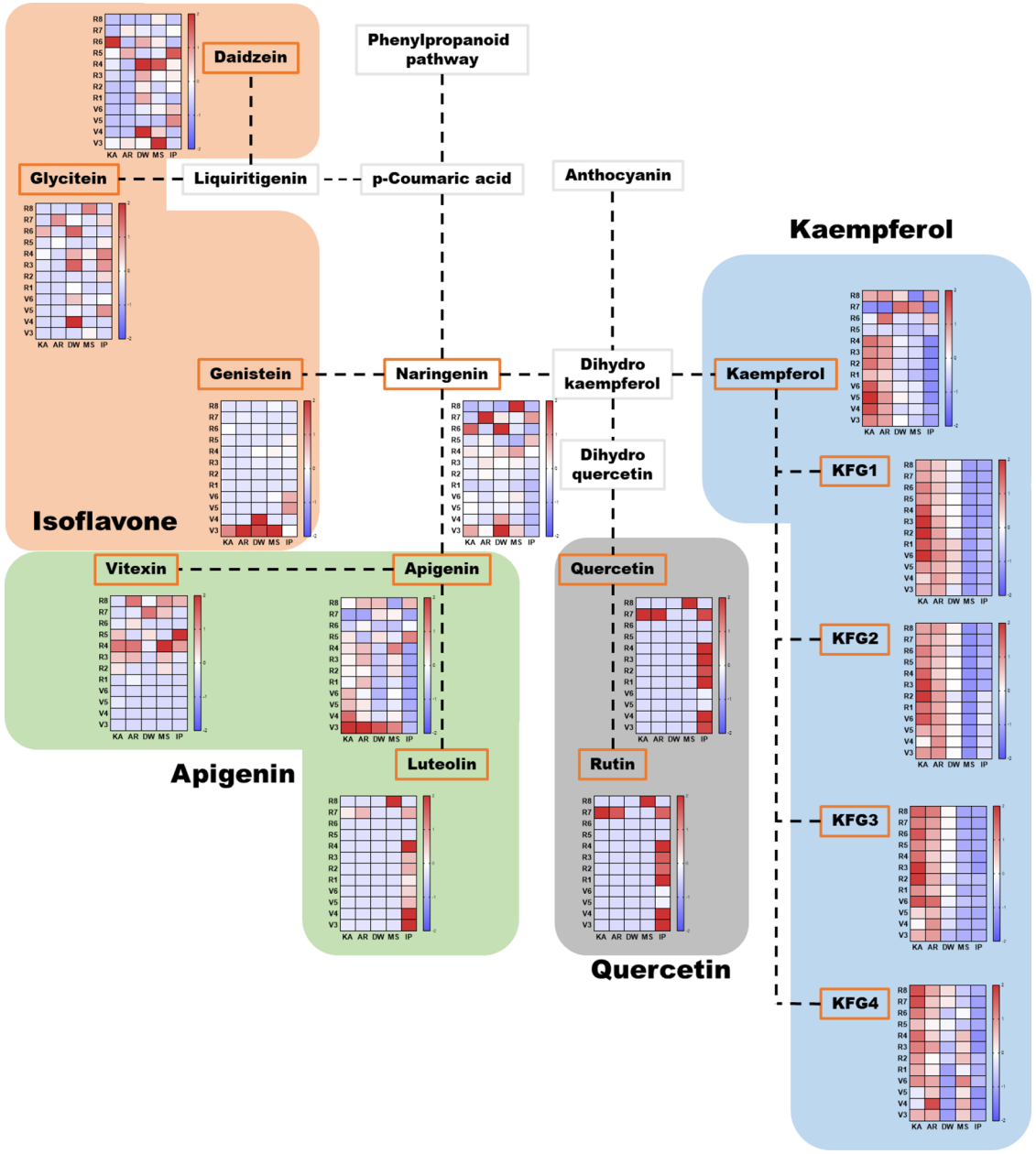

Figure 5. A heatmap representation of flavonoid levels in the five soybean cultivars across the 12 stages. This heatmap shows the levels of flavonoids in a series of metabolic processes in each soybean cultivar across the growth stages. The data of the metabolite contents are normalized by unit variance scaling. The red indicates a high level of flavonoids, and the blue indicates a low level of flavonoids. Abbreviations: KFG1, kaempferol 3-O-(2″-O-glucosyl-6″-O-rhamnosyl)galactoside; KFG2, kaempferol 3-O-(2″-O-glucosyl-6″-O-rhamnosyl)glucoside; KFG3, kaempferol 3-O-(2″-O-glucosyl)-galactoside; KFG4, kaempferol 3-O-(2″-O-glucosyl)glucoside; DW, "Daewon"; IP, "Ilpum"; MS, "Miso"; KA, "Kwangan"; AR, "Aram".

differentially abundant metabolites of soybean leaves from each cultivar. Abbreviations: C28-ol, octacosanol; KF, kaempferol; KFG1, kaempferol 3-O-(2″-O-glucosyl-6″-O-rhamnosyl)-galactoside; KFG2, kaempferol 3-O-(2″-O-glucosyl-6″-O-rhamnosyl)glucoside; KFG3, kaempferol 3-O-(2″-O-glucosyl)-galactoside; KFG4, kaempferol 3-O-(2″-O-glucosyl)glucoside; DW, "Daewon"; IP, "Ilpum"; MS, "Miso"; KA, "Kwangan"; AR, "Aram".

Metabolic Changes in Soybean Leaves among Cultivars. As the initial PCA classified the metabolites according to developmental stage but not by cultivar, we performed an additional PLS-DA to explore differences among cultivars (Figure 4). PLS-DA divided the cultivars into two groups along PLS1 (Figure 4A). AR and KA had positive eigenvalues for PLS1, while IP, MS, and DW had negative eigenvalues for PLS1. We plotted the variable importance in projection (VIP) for those metabolites that showed the greatest cultivar-specific differences across soybean leaves (Figure 4B). In general, VIP values greater than 1 considerably contribute to class separation in PLS modeling.[37] The VIP plot of PLS1 showed large changes in the flavonoid contents as a function of the cultivar. It suggests that variations in flavonoid contents were connected with soybean cultivars rather than growth stages. Furthermore, we focused on the flavonoid pathway to assess the changes in flavonoid contents among the cultivars during all leaf development stages (Figure 5). Kaempferol, the major flavonoid in soybean leaves, highly accumulated in AR and KA. Quercetin,

https://doi.org/10.1021/acsomega.3c06043
ACS Omega 2023, 8, 41718−41727

rutin, and luteolin also highly accumulated during several stages in IP.

Changes in flavonoid metabolism have been observed in soybean leaves based on seed color and growth stage.[38,39] For example, the soybean leaves from yellow soybean seed contained high levels of kaempferol group whereas the soybean leaves from black soybean seed contained high levels of quercetin and isorhamnetin group.[39] Furthermore, variation in the content of isoflavones in soybean seeds depends on their size or weight.[40] The isoflavone pathway is activated in soybean seeds, while the kaempferol pathway is activated in soybean leaves.[10] However, to the best of our knowledge, there are no reports on how seed size affects flavonoid contents in soybean leaves. Cultivars AR and KA have small seeds, while cultivars IP, MS, and DW have large seeds. Furthermore, IP has a black seed coat, whereas the other four cultivars have a yellow seed coat. Small-seeded KA and AR showed remarkably high levels of kaempferol-type metabolites in leaves across most growth stages (Figure 5).

Additionally, KA and AR leaves accumulated more flavonoids than did the other soybean cultivars. IP, with its black seed coat, contained higher amounts of quercetin, rutin, and luteolin in its leaves. Flavonoids are secondary metabolites; their biosynthesis begins with shikimate and phenylalanine.[41] Isoflavone, kaempferol, quercetin, and apigenin all share the same precursor. We observed higher flavonoid contents in leaves from cultivars with smaller seeds. This finding is also supported by supplementary data from previous studies, which showed that cultivars with small seeds have higher kaempferol contents.[39] The high kaempferol content in soybean leaves indicates their potential for strong antioxidant activity. Therefore, the leaves of small-seeded cultivars such as KA and AR may serve as a food source. Black soybean seeds contain high levels of anthocyanins.[42] Anthocyanins share a biosynthetic pathway with kaempferol and quercetin. Cyanidin, the most abundant anthocyanin in black soybeans, is synthesized from dihyroquercetin, a precursor of quercetin. Consequently, we attribute the relatively low kaempferol content and the high quercetin content in black-seeded soybeans to their shared biosynthetic pathway. Taken together, we detected differences in the flavonoid contents of leaves among cultivars and found high levels of kaempferol and total flavonoids in the leaves of the small-seeded cultivars.

In conclusion, we investigated the changes in 72 metabolites across 12 growth stages for five cultivars (KA, AR, MS, DW, and IP) in soybean leaves. We performed multivariate analysis to identify the compounds that separated the samples based on growth stage and cultivar. PCA results revealed that the growth stage strongly influenced the clustering of samples and the PC1 loading plot indicated active carbon-related energy metabolism during the V stages. PLS-DA results unveiled significant alterations in the metabolic networks up to R5, indicating tight coordination between carbon and nitrogen metabolism. Additionally, we observed dramatic changes in the contents of policosilanes, which are major components of the waxy leaf surface. In R6−R8, certain amino acids accumulated, indicating energy redistribution to the seed. Furthermore, we revealed that leaves of cultivars KA and AR are promising sources of flavonoids. Thus, our study demonstrates that the combination of metabolic profiling and chemometrics is an effective approach for monitoring intricate alterations in metabolic networks across various stages of plant development. Recently, Kambhampati et al. analyzed temporal changes in metabolite content throughout soybean seed development.[33] Our future work will focus on analyzing the metabolic profile in soybean seeds and comparing the metabolite content of seeds and leaves from five different cultivars to investigate source−sink interactions.

■ ASSOCIATED CONTENT

Supporting Information

The Supporting Information is available free of charge at https://pubs.acs.org/doi/10.1021/acsomega.3c06043.

Phenotypes of five cultivars of soybeans (KA, Kwangan; AR, Aram; DW, Daewon; IP, Ilpum; MS, Miso) (Figure S1); GC-TOF-MS chromatogram of hydrophilic compounds obtained from soybean leaf (Glycine max (L.) Merr. cv. Kwangan) at R6 stage (Figure S2); GC-qMS chromatogram of lipophilic compounds obtained from soybean leaf (Glycine max (L.) Merr. cv. Kwangan) at R6 stage (Figure S3); UPLC-MS/MS chromatogram of flavonoids obtained from soybean leaf (Glycine max (L.) Merr. cv. Kwangan) at R6 stage (Figure S4); Principal component analysis (PCA) score plot from 72 hydrophilic, lipophilic, and flavonoid compounds of soybean leaves with vegetative growth stages (Figure S5); Retention times and mass spectrometry data of hydrophilic compounds (Table S1); Retention times and mass spectrometry data of lipophilic compounds (Table S2); Retention times and mass spectrometry data of flavonoid compounds (Tables S3) (PDF)

■ AUTHOR INFORMATION

Corresponding Author

Jae Kwang Kim − *Division of Life Sciences, College of Life Sciences and Bioengineering and Convergence Research Center for Insect Vectors, College of Life Sciences and Bioengineering, Incheon National University, Incheon 22012, Republic of Korea;* orcid.org/0000-0003-2692-5370; Email: kjkpj@inu.ac.kr

Authors

Young Jin Park − *Division of Life Sciences, College of Life Sciences and Bioengineering, Incheon National University, Incheon 22012, Republic of Korea*

Jong Sung Lee − *Division of Life Sciences, College of Life Sciences and Bioengineering, Incheon National University, Incheon 22012, Republic of Korea*

Soyoung Park − *Metabolic Engineering Division, National Institute of Agricultural Sciences, Rural Development Administration, Jeonju 54874, Republic of Korea*

Ye Jin Kim − *Division of Life Sciences, College of Life Sciences and Bioengineering, Incheon National University, Incheon 22012, Republic of Korea*

Vimalraj Mani − *Metabolic Engineering Division, National Institute of Agricultural Sciences, Rural Development Administration, Jeonju 54874, Republic of Korea*

Kijong Lee − *Metabolic Engineering Division, National Institute of Agricultural Sciences, Rural Development Administration, Jeonju 54874, Republic of Korea*

Soo Jin Kwon − *Metabolic Engineering Division, National Institute of Agricultural Sciences, Rural Development Administration, Jeonju 54874, Republic of Korea*

Sang Un Park − *Department of Crop Science, Chungnam National University, Daejeon 34134, Republic of Korea;* orcid.org/0000-0003-2157-2246

Complete contact information is available at:

https://doi.org/10.1021/acsomega.3c06043
ACS Omega 2023, 8, 41718−41727

https://pubs.acs.org/10.1021/acsomega.3c06043

Author Contributions

#Y.J.P., J.S.L., and S.P. contributed equally to this work.

Author Contributions

Y.J.P., J.S.L., and S.P. have contributed equally to this work and share first authorship. Y.J.P. performed data curation, formal analysis, writing—original draft, writing—review, and editing. J.S.L. performed methodology, formal analysis, validation, and writing—original draft. S.P. performed methodology, resources, writing—original draft. Y.J.K. performed supervision, writing—review, and editing. V.M. performed resources. K.L. performed conceptualization, resources, supervision, writing—review, and editing. S.J.K. performed conceptualization, resources, supervision. S.U.P. performed supervision. J.K.K. performed conceptualization, supervision, writing—review and editing, project administration.

Notes

The authors declare no competing financial interest.

■ ACKNOWLEDGMENTS

This research was supported by the "Research Program for Agricultural Science & Technology Development, National Academy of Agricultural Science (Project No. PJ01674901)", Rural Development Administration, and the Bio & Medical Technology Development Program of the National Research Foundation (NRF) funded by the Korean government (MSIT) (No. NRF-2022M3H9A2082952), Republic of Korea.

■ ABBREVIATIONS

V stage, vegetative stage; R stage, reproductive stage; DW, *Glycine max* cv. Daewon; IP, *Glycine max* cv. Ilpum; MS, *Glycine max* cv. Miso; KA, *Glycine max* cv. Kwangan; AR, *Glycine max* cv. Aram; PC, principal component; PCA, principal component analysis; PLS-DA, partial least-squares-discriminant analysis; ANOVA, analysis of variance; F6P, fructose-6-phosphate; G6P, glucose-6-phosphate; C22-ol, docosanol; C24-ol, tetracosanol; C26-ol, hexacosanol; C27-ol, heptacosanol; C28-ol, octacosanol; C30-ol, triacontanol; C16:0, palmitic acid; C18:0, stearic acid; KF, kaempferol; KFG1, kaempferol 3-*O*-(2″-*O*-glucosyl-6″-*O*-rhamnosyl)galactoside; KFG2, kaempferol 3-*O*-(2″-*O*-glucosyl-6″-*O*-rhamnosyl)glucoside; KFG3, kaempferol 3-*O*-(2″-*O*-glucosyl)galactoside; KFG4, kaempferol 3-*O*-(2″-*O*-glucosyl)glucoside; MOX, methoxyamine hydrochloride; MSTFA, *N*-methyl-*N*-trimethylsilyl trifluoroacetamide; TCA, tricarboxylic acid; VIP, variable importance in projection; GC-TOF-MS, gas chromatography-time-of-flight-mass spectrometer; GC-qMS, gas chromatography-quadrupole mass spectrometer; UPLC-MS/MS, ultra performance liquid chromatography−tandem mass spectrometer

■ REFERENCES

(1) Kim, Y. J.; Park, Y. J.; Oh, S.-D.; Yoon, J. S.; Kim, J. G.; Seo, J.-S.; Park, J.-H.; Kim, C.-G.; Park, S.-Y.; Park, S. K.; Choi, M.-S.; Kim, J. K. Effects of Genotype and Environment on the Nutrient and Metabolic Profiles of Soybeans Genetically Modified with Epidermal Growth Factor or Thioredoxin Compared with Conventional Soybeans. *Ind. Crops Prod.* **2022**, *175*, No. 114229.

(2) Eskandari, M.; Cober, E. R.; Rajcan, I. Genetic Control of Soybean Seed Oil: II. QTL and Genes that Increase Oil Concentration without Decreasing Protein or with Increased Seed Yield. *Theor. Appl. Genet.* **2013**, *126*, 1677−1687.

(3) Feng, Y.; Ding, Y.; Liu, J.; Tian, Y.; Yang, Y.; Guan, S.; Zhang, C. Effects of Dietary Omega-3/omega-6 Fatty Acid Ratios on Reproduction in the Young Breeder Rooster. *BMC Vet. Res.* **2015**, *11*, 73.

(4) Alam, W.; Khan, H.; Shah, M. A.; Cauli, O.; Saso, L. Kaempferol as a Dietary Anti-Inflammatory Agent: Current Therapeutic Standing. *Molecules* **2020**, *25*, 4073.

(5) Kim, J. K.; Kim, E.-H.; Park, I.; Yu, B.-R.; Lim, J. D.; Lee, Y.-S.; Lee, J.-H.; Kim, S.-H.; Chung, I.-M. Isoflavones Profiling of Soybean [*Glycine max* (L.) Merrill] Germplasms and Their Correlations with Metabolic Pathways. *Food Chem.* **2014**, *153*, 258−264.

(6) Li, H.; Ji, H.-S.; Kang, J.-H.; Shin, D.-H.; Park, H.-Y.; Choi, M.-S.; Lee, C.-H.; Lee, I.-K.; Yun, B.-S.; Jeong, T.-S. Soy Leaf Extract Containing Kaempferol Glycosides and Pheophorbides Improves Glucose Homeostasis by Enhancing Pancreatic β-Cell Function and Suppressing Hepatic Lipid Accumulation in db/db Mice. *J. Agric. Food Chem.* **2015**, *63*, 7198−7210.

(7) Yang, Y.; Chen, Z.; Zhao, X.; Xie, H.; Du, L.; Gao, H.; Xie, C. Mechanisms of Kaempferol in the Treatment of Diabetes: A Comprehensive and Latest Review. *Front. Endocrinol.* **2022**, *13*, No. 990299, DOI: 10.3389/fendo.2022.990299.

(8) Chen, A. Y.; Chen, Y. C. A Review of the Dietary flavonoid, Kaempferol on Human Health and Cancer Chemoprevention. *Food Chem.* **2013**, *138*, 2099−2107.

(9) Yun, D.-Y.; Kang, Y.-G.; Kim, M.; Kim, D.; Kim, E.-H.; Hong, Y.-S. Metabotyping of Different Soybean Genotypes and Distinct Metabolism in Their Seeds and Leaves. *Food Chem.* **2020**, *330*, No. 127198.

(10) Ho, H. M.; Chen, R. Y.; Leung, L. K.; Chan, F. L.; Huang, Y.; Chen, Z.-Y. Difference in flavonoid and isoflavone Profile between Soybean and Soy Leaf. *Biomed. Pharmacother.* **2002**, *56*, 289−295.

(11) Fehr, W. R.; Caviness, C. E. *Stages of Soybean Development Iowa Agricultural and Home Economics Experiment Station Special Report* **1977**, *80*, 3−11.

(12) Seo, W. D.; Kang, J. E.; Choi, S.-W.; Lee, K.-S.; Lee, M.-J.; Park, K.-D.; Lee, J. H. Comparison of Nutritional Components (isoflavone, Protein, Oil, and Fatty Acid) and Antioxidant Properties at the Growth Stage of Different Parts of Soybean [*Glycine max* (L.) Merrill]. *Food Sci. Biotechnol.* **2017**, *26*, 339−347.

(13) Yuk, H. J.; Curtis-Long, M. J.; Ryu, H. W.; Jang, K. C.; Seo, W. D.; Kim, J. Y.; Kang, K. Y.; Park, K. H. Pterocarpan Profiles for Soybean Leaves at Different Growth Stages and Investigation of Their Glycosidase Inhibitions. *J. Agric. Food Chem.* **2011**, *59*, 12683−12690.

(14) Lee, J. H.; Ha, T. J.; Baek, I.-Y.; Ko, J.-M.; Cho, K. M.; Im, M.-H.; Choung, M.-G. Characterization of Isoflavones Accumulation in Developing Leaves of Soybean (*Glycine max*) Cultivars. *J. Appl. Biol. Chem.* **2009**, *52*, 139−143.

(15) Yun, D.-Y.; Kang, Y.-G.; Yun, B.; Kim, E.-H.; Kim, M.; Park, J. S.; Lee, J. H.; Hong, Y.-S. Distinctive Metabolism of flavonoid between Cultivated and Semiwild Soybean Unveiled through Metabolomics Approach. *J. Agric. Food Chem.* **2016**, *64*, 5773−5783.

(16) Kim, T. J.; Hyeon, H.; Park, N. I.; Yi, T. G.; Lim, S.-H.; Park, S.-Y.; Ha, S.-H.; Kim, J. K. A High-throughput Platform for Interpretation of Metabolite Profile Data from Pepper (*Capsicum*) Fruits of 13 Phenotypes Associated with Different Fruit Maturity States. *Food Chem.* **2020**, *331*, No. 127286.

(17) Kopka, J.; Fernie, A.; Weckwerth, W.; Gibon, Y.; Stitt, M. Metabolite Profiling in Plant Biology: Platforms and Destinations. *Genome Biol.* **2004**, *5*, 109.

(18) Tikunov, Y.; Lommen, A.; de Vos, C. H. R.; Verhoeven, H. A.; Bino, R. J.; Hall, R. D.; Bovy, A. G. A Novel Approach for Nontargeted Data Analysis for Metabolomics. Large-Scale Profiling of Tomato Fruit Volatiles. *Plant Physiol.* **2005**, *139*, 1125−1137.

(19) Zhao, H.; Liu, Y.; Huang, Y.; Liang, Q.; Cai, S.; Zhang, G. Time-Course Comparative Metabolome Analysis of Different Barley Varieties during Malting. *J. Agric. Food Chem.* **2022**, *70*, 2051−2059.

(20) Jung, J.-W.; Park, S.-Y.; Oh, S.-D.; Jang, Y.; Suh, S.-J.; Park, S.-K.; Ha, S.-H.; Park, S.-U.; Kim, J.-K. Metabolomic Variability of Different Soybean Genotypes: β-Carotene-Enhanced (*Glycine max*), Wild

(*Glycine soja*), and Hybrid (*Glycine max* × *Glycine soja*) Soybeans. *Foods* **2021**, *10*, 2421.
(21) Shu, X.-L.; Frank, T.; Shu, Q.-Y.; Engel, K.-H. Metabolite Profiling of Germinating Rice Seeds. *J. Agric. Food Chem.* **2008**, *56*, 11612−11620.
(22) Baek, S.-A.; Im, K.-H.; Park, S. U.; Oh, S.-D.; Choi, J.; Kim, J. K. Dynamics of Short-Term Metabolic Profiling in Radish Sprouts (*Raphanus sativus* L.) in Response to Nitrogen Deficiency. *Plants* **2019**, *8*, 361.
(23) Baek, S.-A.; Kim, K. W.; Kim, J. O.; Kim, T. J.; Ahn, S. K.; Choi, J.; Kim, J.; Ahn, J.; Kim, J. K. Metabolic Profiling Reveals an Increase in Stress-related Metabolites in *Arabidopsis thaliana* Exposed to Honeybees. *J. Appl. Biol. Chem.* **2021**, *64*, 141−151.
(24) Kim, T. J.; Lee, K. B.; Baek, S.-A.; Choi, J.; Ha, S.-H.; Lim, S.-H.; Park, S.-Y.; Yeo, Y.; Park, S. U.; Kim, J. K. Determination of Lipophilic Metabolites for Species Discrimination and Quality Assessment of Nine Leafy Vegetables. *J. Korean Soc. Appl. Bio. Chem.* **2015**, *58*, 909−918.
(25) Jung, J. W.; Oh, S.-D.; Park, S.-Y.; Jang, Y.; Lee, S.-K.; Yun, D.-W.; Chang, A.; Park, S. U.; Ha, S.-H.; Kim, J. K. Metabolic Profling and Antioxidant Properties of Hybrid Soybeans with Different Seed Coat Colors, Obtained by Crossing β-Carotene-enhanced (*Glycine max*) and Wild (*Glycine soja*) Soybeans. *Plant Biotechnol. Rep.* **2022**, *16*, 449−463.
(26) Zhou, H.; Xu, M.; Pan, H.; Yu, X. Leaf-age Effects on Temperature Responses of Photosynthesis and Respiration of an Alpine Oak, Quercus Aquifolioides, in Southwestern China. *Tree Physiol.* **2015**, *35*, 1236−1248.
(27) Makino, A.; Mae, T.; Ohira, K. Photosynthesis and Ribulose 1,5-Bisphosphate Carboxylase in Rice Leaves: Changes in Photosynthesis and Enzymes Involved in Carbon Assimilation from Leaf Development through Senescence. *Plant Physiol.* **1983**, *73*, 1002−1007.
(28) Koch, K. Sucrose Metabolism: Regulatory Mechanisms and Pivotal Roles in Sugar Sensing and Plant Development. *Curr. Opin. Plant Biol.* **2004**, *7*, 235−246.
(29) Kim, K. S.; Park, S. H.; Kim, D. K.; Jenks, M. A. Influence of Water Deficit on Leaf Cuticular Waxes of Soybean (*Glycine max* [L.] Merr.). *Int. J. Plant Sci.* **2007**, *168*, 307−316.
(30) Guo, J.; Xu, W.; Yu, X.; Shen, H.; Li, H.; Cheng, D.; Liu, A.; Liu, J.; Liu, C.; Zhao, S.; Song, J. Cuticular Wax Accumulation Is Associated with Drought Tolerance in Wheat Near-isogenic Lines. *Front. Plant Sci.* **2016**, *7*, 1809 DOI: 10.3389/fpls.2016.01809.
(31) Shalit-Kaneh, A.; Eviatar-Ribak, T.; Horev, G.; Suss, N.; Aloni, R.; Eshed, Y.; Lifschitz, E. The Flowering Hormone Florigen Accelerates Secondary Cell Wall Biogenesis to Harmonize Vascular Maturation with Reproductive Development. *Proc. Natl. Acad. Sci. U. S. A.* **2019**, *116*, 16127−16136.
(32) Ohyama, T.; Ohtake, N.; Sueyoshi, K.; Ono, Y.; Tsutsumi, K.; Ueno, M.; Tanabata, S.; Sato, T.; Takahashi, Y. Amino Acid Metabolism and Transport in Soybean Plants. In Asao, T., Asaduzzaman, M. (Eds.), *Amino Acid − New Insights and Roles in Plant and Animal*; IntechOpen, 2017.
(33) Kambhampati, S.; Aznar-Moreno, J. A.; Bailey, S. R.; Arp, J. J.; Chu, K. L.; Bilyeu, K. D.; Durrett, T. P.; Allen, D. K. Temporal Changes in Metabolism Late in Seed Development Affect Biomass Composition. *Plant Physiol.* **2021**, *186*, 874−890.
(34) Develey-Rivière, M.-P.; Galiana, E. Resistance to Pathogens and Host Developmental Stage: A Multifaceted Relationship within the Plant Kingdom. *New Phytol.* **2007**, *175*, 405−416.
(35) Dufourc, E. J. The Role of Phytosterols in Plant Adaptation to Temperature. *Plant Signal. Behav.* **2008**, *3*, 133−134.
(36) Mohsen, S. M.; Fadel, H. H. M.; Bekhit, M. A.; Edris, A. E.; Ahmed, M. Y. S. Effect of Substitution of Soy Protein Isolate on Aroma Volatiles, Chemical Composition and Sensory Quality of Wheat Cookies. *Int. J. Food Sci. Technol.* **2009**, *44*, 1705−1712.
(37) Weidong, Z.; Sergei, L.; Yuhua, Z.; Erfan, A.-E.; Patricia, E. H.; Edward, R.; Roger, G.; Glynn, M.; Andrew, F.; Guang, S.; Proton, R.; Guangju, Z. Classification of Osteoarthritis Phenotypes by Metabolomics Analysis. *BMJ. Open* **2014**, *4*, No. e006286.
(38) Song, H.-H.; Ryu, H. W.; Lee, K. J.; Jeong, I. Y.; Kim, D. S.; Oh, S.-R. Metabolomics Investigation of flavonoid Synthesis in Soybean Leaves Depending on the Growth Stage. *Metabolomics* **2014**, *10*, 833−841.
(39) Lee, S.; Kim, H.-W.; Lee, S.-J.; Kwon, R. H.; Na, H.; Kim, J. H.; Choi, Y.-M.; Yoon, H.; Kim, Y.-S.; Wee, C.-D.; Yoo, S. M.; Lee, S. H. Comprehensive Characterization of flavonoid Derivatives in Young Leaves of Core-collected Soybean (*Glycine max* L.) Cultivars based on High-resolution Mass Spectrometry. *Sci. Rep.* **2022**, *12*, 14678.
(40) Lee, S.-J.; Kim, J.-J.; Moon, H.-I.; Ahn, J.-K.; Chun, S.-C.; Jung, W.-S.; Lee, O.-K.; Chung, I.-M. Analysis of Isoflavones and Phenolic Compounds in Korean Soybean [*Glycine max* (L.) Merrill] Seeds of Different Seed Weights. *J. Agric. Food Chem.* **2008**, *56*, 2751−2758.
(41) Vogt, T. Phenylpropanoid Biosynthesis. *Mol. Plant* **2010**, *3*, 2−20.
(42) Krishnan, V.; Rani, R.; Pushkar, S.; Lal, S. K.; Srivastava, S.; Kumari, S.; Vinutha, T.; Dahuja, A.; Praveen, S.; Sachdev, A. Anthocyanin Fingerprinting and Dynamics in Differentially Pigmented Exotic Soybean Genotypes using modified HPLC−DAD Method. *J. Food Meas. Charact.* **2020**, *14*, 1966−1975.

https://doi.org/10.1021/acsomega.3c06043
ACS Omega 2023, 8, 41718−41727